Marine nanogels as a source of atmospheric nanoparticles in the high Arctic

Matthias Karl,[1] Caroline Leck,[2] Esther Coz,[3] and Jost Heintzenberg[4]

Received 21 May 2013; revised 9 June 2013; accepted 13 June 2013; published 19 July 2013.

[1] The high Arctic (north of 80°N) in summer is a region characterized by clean air and low abundances of preexisting particles. Marine colloidal nanogels i.e., assembled dissolved organic carbohydrate polymer networks have recently been confirmed to be present in both airborne particles and cloud water over the Arctic pack ice area. A novel route to atmospheric nanoparticles that appears to be operative in the high Arctic is suggested. It involves the injection of marine granular nanogels into the air from evaporating fog and cloud droplets, and is supported by observational and theoretical evidence obtained from a case study. Statistical analysis of the aerosol size distribution data recorded in the years 1991, 1996, 2001, and 2008 classified 75 nanoparticle events—covering 17% of the observed time period—as nanogel-type events, characterized by the spontaneous appearance of several distinct size bands below 200 nm diameter. **Citation:** Karl, M., C. Leck, E. Coz, and J. Heintzenberg (2013), Marine nanogels as a source of atmospheric nanoparticles in the high Arctic, *Geophys. Res. Lett.*, *40*, 3738–3743, doi:10.1002/grl.50661.

1. Introduction

[2] The high Arctic summer (at latitude >80°N) atmosphere is of particular interest for the study of aerosol-cloud-climate interactions, since it is characterized by relatively few aerosol particles, usually less than 150 per cubic centimeter (cm^{-3}), available to form cloud droplets [*Bigg et al.*, 1996] and by only few sources of aerosol particles [*Leck and Persson*, 1996]. Nucleation mode (diameter 3–25 nm) and Aitken mode particles (diameter 25–80 nm) have been demonstrated to be produced by in situ fine-particle sources over the high Arctic pack ice and possibly have a marine biological origin in the open water between ice floes [*Heintzenberg et al.*, 2006; *Heintzenberg and Leck*, 2012].

[3] High Arctic nanoparticle events are characterized by simultaneous number enhancement in distinct size ranges [*Leck and Bigg*, 1999, 2010; *Karl et al.*, 2012] not following the banana-shaped growth curve typical for continental nucleation events [*Kulmala and Kerminen*, 2008]. The observed coappearance of particles in the 20–50 nm diameter size range coinciding with nucleation in many cases could not be explained by secondary particle formation [*Karl et al.*, 2012]. *Covert et al.* [1996] detected frequent abundance of particles in the 2.7–5 nm size range in the high Arctic atmospheric boundary layer (BL). However, as shown by *Karl et al.* [2012], the rapid appearance of 3–8 nm particles cannot be explained as a result of the growth of the freshly nucleated stable clusters of 1–2 nm diameter by a semi-volatile condensable organic vapor (COV) essentially because the Kelvin effect imposes a giant barrier for the initial growth [*Karl et al.*, 2011]. In addition, it was shown that the availability of condensable vapors is limited in the atmospheric BL over the inner Arctic; and the concentration of dimethyl sulfide (DMS), precursor to sulfuric acid (H_2SO_4), is often not sufficient to sustain growth into the 3–8 nm diameter size range.

[4] Marine gels span the whole size spectrum from ~2–10 nm diameter (colloidal nanogels) containing single macromolecules, up to micrometer-sized gels (colloidal microgels) that can aggregate to several hundred μm (macrogels). *Verdugo* [2012] gives a review. For the first time, *Orellana et al.* [2011] applied a highly specific antibody developed against seawater biopolymers to cloud, fog, and aerosol particle samples collected over the pack ice in summer. These tests confirmed that both the airborne and cloud/fog nanogels and microgels originated in the surface micro layer (SML) of the open leads. The significance of the very large numbers of nanoparticles of marine biological origin, hereafter referred to as *nano-granules*, in airborne aerosol during episodes with enhanced particle numbers was first recognized by *Leck and Bigg* [1999, 2010]. Relating to the circumstance that the onset of central Arctic Ocean nanoparticle events often occurs short after dissipation of fog [*Heintzenberg and Leck*, 1994; *Leck and Bigg*, 1999, 2010; *Karl et al.*, 2012], we propose here that fog and cloud droplets are a medium facilitating the collapse of the marine gels which enclosed the nano-granules.

[5] Inspired by the observations and suggestions discussed above, a novel route to new atmospheric nanoparticles (illustrated in Figure 1) over the pack ice area in summer is outlined as follows: (1) release of nano-granules from evaporating fog/cloud droplets, (2) nucleation of H_2SO_4 molecules to form stable clusters, (3) condensation of low-volatile vapors onto both the granules and the H_2SO_4 clusters, (4) coagulation of granules and H_2SO_4 clusters to form > 3 nm diameter sized particles. We tested the above hypotheses in a "clean air" case study of a nanoparticle event observed at latitude 87°N when concentrations of precursor gases (e.g., DMS and isoprene) were very low [*Kupiszewski*

Additional supporting information may be found in the online version of this article.

[1]NILU-Norwegian Institute for Air Research, Kjeller, Norway.
[2]Department of Meteorology, Stockholm University, Stockholm, Sweden.
[3]Department of Environment, CIEMAT, Madrid, Spain.
[4]Leibniz Institute for Tropospheric Research, Leipzig, Germany.

Corresponding author: M. Karl, Department for Urban Environment and Industry, NILU-Norwegian Institute for Air Research, NO-2027 Kjeller, Norway. (mka@nilu.no)

0094-8276/13/10.1002/grl.50661

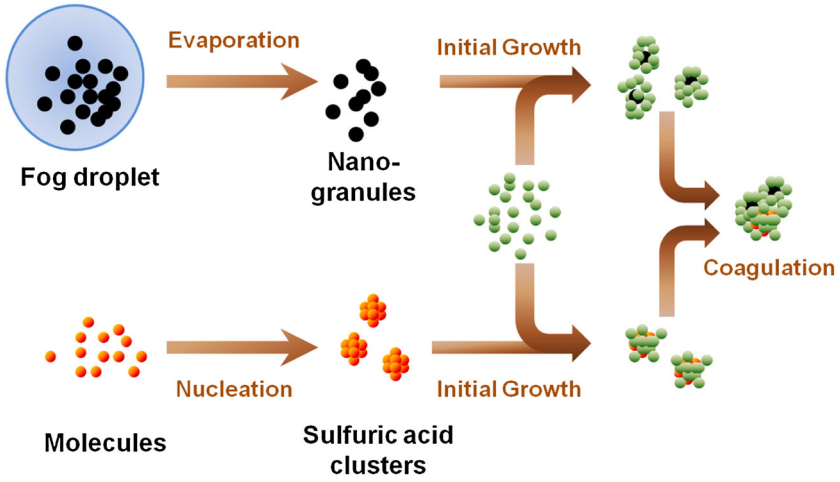

Figure 1. Schematic outline of the suggested route to new atmospheric nanoparticles, involving sulfuric acid (orange), organic vapor (green), and marine nano-granules (black).

et al., 2013]; adding a barrier for the initial growth of new particles. We combined the results from (1) quantitatively derived size-resolved electron microscope mapping of nanogels in air, fog/cloud water and in the SML collected in situ, (2) model simulations to study the relevance of aerosol processes during the event, and (3) statistical analysis of the temporal development of all previously observed high Arctic nanoparticle events.

2. Methods

[6] The measurements of airborne aerosol particles, fog/cloud water, and the SML water were performed as part of the activities of the research program on the Arctic Summer Cloud and Ocean Study (ASCOS) onboard the Swedish icebreaker *Oden* in 2008 [*Tjernström et al.*, 2013]. The measurement of number size distributions of dry submicrometer particles by a Twin Differential Mobility Particle Sizer (TDMPS) system and the measurement of gas phase DMS are described in the supporting information, section S1. The samples (air, low-level cloud water, and SML) were collected simultaneously before and during the nanoparticle event. Morphology and number size distribution of nano-granules and colloidal nanogels were determined as described in the supporting information, section S2.

[7] To perform simulations of the new particle event, the sectional aerosol box model Marine Aerosol Formation model, version 1.6 [*Karl et al.*, 2011] (http://mafor.nilu.no), was applied. The growth of particles in the model occurs through multicomponent condensation of H_2SO_4, methane sulphonic acid (MSA), and COV. The Fuchs-Sutugin expression for condensation was modified according to *Lehtinen and Kulmala* [2003]. Since the identity of the COV causing

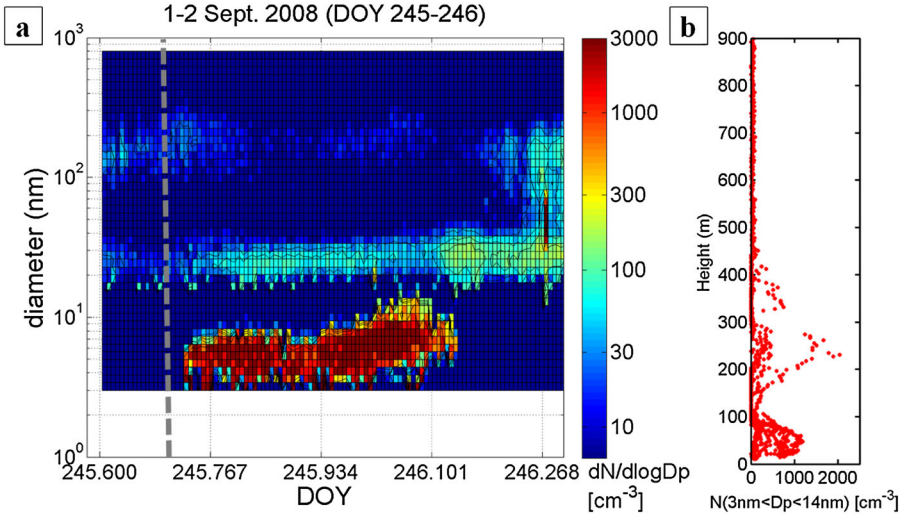

Figure 2. Number enhancement of nanoparticles on DOY 245–246: (a) Sequential aerosol size distribution of the event measured by TDMPS, (b) vertical profile of the number concentration of particles with 3 nm< D_p <14 nm recorded by ultrafine condensation particle counter (UCPC) during helicopter flight DOY 245.820–245.840. For more details on the vertical profiling, see *Kupiszewski et al.* [2013]. The fog preceding the nanoparticle event started at DOY 245.380 and ended at DOY 245.702 (marked by horizontal dashed gray line in Figure 2a). The nanoparticle event started at DOY 245.727 and ended at DOY 246.101.

the growth is unknown, a zero surface pressure on the particles was assumed. The diameter size range between 1 nm and 10 nm was resolved with 30 logarithmically spaced size bins.

3. Results

[8] An episode with vigorous number enhancement of nanoparticles was observed during DOY 245–246 (01 and 02 September 2008; at 87.1°N; 12°W). The onset of the event was associated with rapid dissipation of intermittent low-level cloud (fog) at DOY 245.702. Figure 2a shows the sequential number size distributions during the event. The meteorological conditions during the event are described in the supporting information, section S3.

[9] Newly formed particles (<15 nm diameter), seen by the TDMPS (Figure 2), were confined within the shallow layer below 150 m (Figure 2b). This layer was capped with a strong inversion and a stable layer of ~1 km in depth, excluding an upper tropospheric particle source (Figure S2). The layer between 100 m and 300–400 m shows the remnants of the mixing by the low cloud layer and contained up to ~ 600 cm^{-3} particles with sizes <14 nm (Figure 2b). Only weak signs of elevated nucleation mode particles were observed above 400 m altitude [*Kupiszewski et al.*, 2013].

[10] The water insoluble organic material in the low-level cloud water samples contained 10^{11} nanogels per cm^2, ranging from 1 to several nanometer sizes. The nanogels formed 3-D net arrays in the background of the substrates in overloaded areas (Figures 3a and 3b). Figure 3c representing the SML shows the presence of electron-opaque aggregates of colloidal gels within an almost electron transparent film or mucus holding the aggregates together in rafts or strings, resembling earlier work by *Bigg et al.* [2004] in the same area and season. The airborne representative (Figure 3d) was dominated by colloids and had apparently lost its surrounding mucus-like film once airborne.

[11] Four cases were simulated with the model; Case 1: nucleation and growth by H_2SO_4 and COV, Case 2: emission of marine nanogels in nucleation and Aitken mode, Case 3: combination of nucleation, growth, and marine nanogel emission, and Case 4: as Case 3 but without nucleation. Details of the model configurations are provided in Table 1. It was assumed that initially zero particles were present. Initial H_2SO_4 concentration has been set to 1×10^6 cm^{-3}, an upper limit for high Arctic BL air [*Karl et al.*, 2011, 2012].

[12] Case 1 (secondary particle formation) enabled growth of nucleated particles to final sizes of about 10 nm (Figure 4a). The prescribed COV concentration of 4×10^7 cm^{-3} (~1.5 pptv) was an upper limit value constrained by the observed growth rate in the second half of the event (~0.5 nm h^{-1}). The low-level cloud (fog) evaporated short before the event start (t_1), leaving freshly nucleated particles approximately 0.5 h to grow into sizes > 3 nm diameter by condensation. Measured number concentration of 3–10 nm particles (N_{10}) had a first maximum ~1.5 h and a second one ~7 h after event start (Figure S3). In Case 1, particles >3 nm appeared with a delay of 1.5 h after the observed event start. The first N_{10} peak was not captured but the second N_{10} peak was reproduced (Figure S3). The delayed onset in Case 1 was also evident when considering uncertainties in the initial concentrations of H_2SO_4, DMS, and particles, nucleation rate and growth rate (Figure S4).

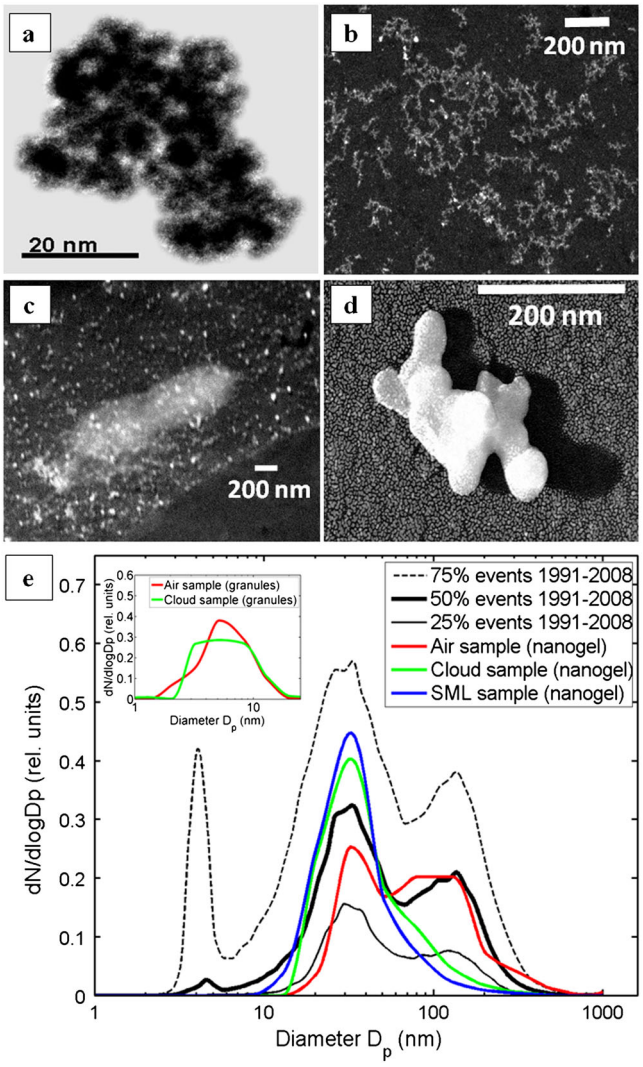

Figure 3. Nanocolloids (a and b) in the cloud sample, (c) in the open lead SML sample, and (d) in the air sample obtained by microscope image processing. (e) Colloidal gel size distributions of the air, cloud and SML samples (normalized by total number of colloids) obtained by microscope image processing, and the statistics of relative number size distributions during the nanogel-type events (75%, 50%, and 25% percentile) in 1991, 1996, 2001, and 2008 (see text for details). Inset shows the nano-granular distribution (1–25 nm diameter range) in the air and cloud samples.

[13] In Case 2, a constant source of nanogels was considered, while secondary particle formation was not allowed. To our knowledge, the number flux of nanoparticles from evaporating low-level cloud (fog) has not been quantified previously. Number flux, F_N, and geometric mean diameter, *GMD*, of emitted particles were thus derived by matching the observed aerosol size distribution at t_1 (see Table 1). Case 2 simulation compared well with the observed total number concentrations but did not reproduce the growth observed after DOY 245.93 (Figure 4b).

[14] Case 3, the combination of secondary production and emission (using flux parameters from Case 2), resulted a much better agreement in the second half of the event (Figure 4c). The starting time of COV condensation (DOY 245.917) in this simulation was motivated by the observed

Table 1. Processes and Parameters of the Four Model Configurations: (1) Nucleation and Growth Alone, (2) Emission of Nano-Granules, (3) Nucleation and Growth Together With Emission of Nano-Granules, and (4) Growth and Emission of Nano-Granules

Model Process	Case 1	Case 2	Case 3	Case 4
Nucleation	combined H_2SO_4[c]	—	combined H_2SO_4[c]	—
	A= $2.4\times10^{-7}s^{-1}$	—	A= $2.4\times10^{-7}s^{-1}$	—
Condensation	H_2SO_4, MSA	—	H_2SO_4, MSA	
	COV prescribed.	—	COV prescribed after DOY 245.917.	
	[COV]= $4\times10^{7}cm^{-3}$	—	[COV]=$4\times10^{7}cm^{-3}$	
	p^s(COV) = 0 Pa	—	p^s(COV)=0 Pa	
Emission[a,b]	—		nano-granules	
F_N(Nu1)	—		9.4×10^{6}	
F_N(Nu2)	—		0.21×10^{6}	
GMD(Nu1)	—		4.5nm	
GMD(Nu2)	—		25.5nm	

[a] Emission of nonhygroscopic biological particles in the first and second nucleation mode (Nu1 and Nu2) with average density of 1150 kg m^{-3} and bandwidth (σ_p) of 1.10.

[b] Number flux (F_N) in unit $m^{-2}s^{-1}$ and geometric mean diameter (GMD) were adjusted to match observed number concentrations and diameter 1 h after event start in Case 2. In Case 3, the emission parameters derived in Case 2 were applied.

[c]Details of the combined nucleation mechanism are given in *Karl et al.* [2011]. Nucleation rate is calculated as $J=A[H_2SO_4]+J_{IMN}$; where J_{IMN} is the nucleation rate of the ion-mediated mechanism assuming quasi steady state conditions for the charged clusters. The combined nucleation mechanism has been found to predict observed maximum nucleation mode numbers during the high Arctic events within a factor of 2 – 3, see *Karl et al.* [2012].

appearance of organic vapors (e.g., ∼20 pptv isoprene was measured, Figure S3; unpublished PTR-ToF-MS data, M. Graus, 2009). Coagulation of H_2SO_4 clusters with the larger nano-granules was of little relevance; the coagulation sink of 1 nm clusters ($\sim5\times10^{-6}$ s^{-1} being two orders of magnitude smaller than their condensation sink ($\sim5\times10^{-4}$ s^{-1}). The competition for available COV had negligible effect on the growth rate of the clusters. Not allowing nucleation of H_2SO_4 clusters (Case 4) resulted in similar temporal evolution of the size distribution of >3 nm particles (Figure S5). However, we note that sub-3 nm diameter clusters are likely present even at very low H_2SO_4 concentrations [*Kulmala et al.*, 2013]; thus, case 4 is less realistic. Modeled time series of N_{10} in cases 2–4 during the event were in agreement with the observed time series N_{10} (Figure S3). The observed number size distribution (Figure 4d) could be reproduced with the model when a combination of secondary particle formation and nanogel emission was considered.

[15] A statistical analysis was performed to identify and analyze nanoparticle events in the combined hourly TDMPS records of the four available Arctic *Oden* cruises in the years 1991, 1996, 2001, and 2008 (details in the supporting information, section S5). The 75 events were identified by a factor of two or higher increases in total number after onset, covering 17% of the total time period. These events were characterized by almost complete absence of preevent particles and by the immediate increase of number concentrations in practically all sizes up to 200 nm diameter, with the exception of a gap around 6 nm that widens to ∼10 nm (Figure S7).

[16] At all times during the events, modes or relative maxima are found in several discrete bands. We interpret these events as appearance of airborne nanogel particles after dissipation of fog or cloud. This is further supported by the almost perfect match of Aitken mode diameter in the 25%, 50%, and 75% percentile of the average event size distribution with the peak at ∼30 nm diameter in the air, cloud, and SML samples (Figure 3e; Table S1). The colloidal size distribution derived from the microscope images of the air sample (red line in Figure 3e) reproduces the bimodality fea-

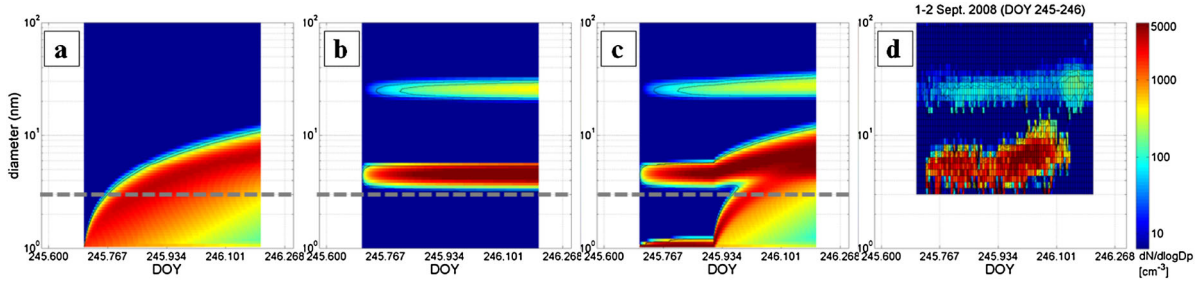

Figure 4. Temporal evolution of the size distribution (below 100 nm) during the nanoparticle event: (a) model simulation Case 1: secondary particle formation by nucleation and condensational growth using a prescribed COV concentration of 4×10^{7} cm^{-3}, (b) model simulation Case 2: emission of nanogels using constant particle number fluxes of 9.4×10^{6} m^{-2} s^{-1} at mean diameter of 4.5 nm and 0.21×10^{6} m^{-2} s^{-1} at mean diameter of 25.5 nm, (c) model simulation Case 3: nucleation, condensation, and emission by combination of Case 1 and Case 2, (d) measurement by TDMPS for comparison (same as Figure 2a but only the time period of the event). Horizontal dashed gray line marks 3 nm diameter.

ture of the average event size distribution and of the TDMPS size distribution shown in Figure 2, with peaks at ∼30 nm and at ∼160 nm diameter. The nano-granule peak below 10 nm size was found in the cloud and in the air sample (inset in Figure 3e).

4. Discussion

[17] The significant presence of nm-sized marine gels in the low-level cloud water preceding the nanoparticle event, and our model simulation of the event, reemphasize past suggestions [*Leck and Bigg*, 1999, 2010] of a link between evaporating clouds containing water insoluble and positively net charged colloidal nanogels of marine biological origin [*Orellana et al.*, 2011] and new atmospheric nanoparticles. While the formation of high-MW oligomers from glyoxal and glycolaldehyde in the liquid phase [e.g., *De Haan et al.*, 2009] during droplet evaporation may serve as an alternative explanation for particle formation in vicinity of clouds, we assume that the residual particles from this process are larger than 10 nm since they would also include sulfate that formed as result of aqueous-phase reactions in the droplet [*Pandis et al.*, 1990]. Therefore, we find this possibility less likely to explain our results. Free charge can cause fragmentation of fog/cloud droplets when the evaporating droplet radius approaches the Rayleigh stability limit [*Kozyrev and Sitnikov*, 2003], leading to the ejection of highly charged small droplets. *Leck and Bigg* [1999] suggested that disruption of particles by electric charge might provide an appropriate mechanism explaining the remote summer Arctic nanoparticle events. As being addressed more recently by *Leck and Bigg* [2010]: if Rayleigh explosions occur at all, a prime place for them would be at the top or outflow from marine cumulus clouds, or in regions where evaporating cloud drops occur. If valid, this process could have explained the layers of <5 nm particles observed from an aircraft in the free troposphere in a cloudy region over a biologically productive part of an equatorial ocean by *Clarke et al.* [1998]. Direct eddy covariance measurements during the ASCOS expedition showed that aerosol number fluxes from the open leads, dominated by particles in the sub-50 nm diameter range, were below 0.1×10^6 m^{-2} s^{-1} [*Held et al.*, 2011]; only weakly contributing to atmospheric particle numbers. The occurrence of two distinct modes (at ∼3–4 nm and ∼20–50 nm; Figure 3e) might be explained by the 3-D polymer network structure of the nanogels. In the aqueous phase, the continuous assembly/dispersion equilibrium of nm-sized gels can be affected by environmental parameters, such as UV-B radiation (λ = 280–320 nm), pH, and temperature changes, breaking up the nanogel polymer network [*Verdugo*, 2012]. Calculating the number flux of 20–50 nm primary particles according to the sea spray parameterization by *Mårtensson et al.* [2003] for average conditions during the event (U_{10} = 5.5 m s^{-1}, T_{sea} = 271.5 K) resulted in 1.06×10^5 m^{-2} s^{-1}. Assuming that half of the emitted population breaks up into spherical 5 nm units by in-cloud processes or during droplet evaporation, the number flux is 2.0×10^7 m^{-2} s^{-1}, two times higher than the flux of nano-granules required to simulate the event. However, transferring the parameterization to open lead fluxes remains questionable because it has been derived from experiments with pure saline water, not having an organic SML. We note that in our study, airborne biological particles were assumed to be nonhygroscopic and insoluble in water. Despite their hydrophobic character, primary organic particles were found to have higher activation efficiency than more soluble inorganic aerosol [*Ovadnevaite et al.*, 2011], probably due to strong surfactant properties of the marine gels. Hence, nanogels could furthermore serve as cloud condensation nuclei by lowering the surface tension of the droplets.

5. Conclusions

[18] In this paper, observational and theoretical evidence is presented in support of a novel route to new atmospheric nanoparticles in the high Arctic, involving the injection of biogenic granular nanogels into the air from evaporating clouds. The co-occurrence of atmospheric organic material resembling gel-polysaccharides and biologically active marine waters has been confirmed for the high Arctic waters [*Orellana et al.*, 2011] and has also been documented for temperate waters [*Facchini et al.*, 2008; *Russel et al.*, 2010; *Leck and Bigg*, 2008]. However, more samples both from the coastal and open water regions of the Arctic Ocean and at lower latitude oceans have to be collected and analyzed before conclusions on the universality of such nanogels and microgels can be drawn.

[19] **Acknowledgments.** B. Wehner and D. Orsini are much appreciated for providing the size-resolved particle number observations. S. Sjogren and L. Orr are thanked for the helicopter data. The authors thank L. Pirjola for critical remarks. Special thanks must go to K. Jansson and A. Öhrström for their long hours imaging the marine gels using the electron microscopes. The AEROCLIMA project (Fundación Ramón Areces) contributed high resolution TEM analyses conducted at the National Center for electron Microscopy, UCM (Madrid, Spain). The Swedish Polar Research Secretariat (SPRS) provided access to the icebreaker *Oden* and logistical support. We are grateful to the SPRS logistical staff and to *Oden*'s Captain M. Peterson and his crew. Michael Tjernström is specifically thanked for his co-coordination of ASCOS. ASCOS is an IPY project under the AICIA-IPY umbrella and an endorsed SOLAS project. The Swedish Research Council, the Knut and Alice Wallenberg Foundation, the DAMOCLES European Union 6th Framework Program Integrated Research Project, and the International Institute of Meteorology provided support for this work.

[20] The Editor thanks Lynn Russell and an anonymous reviewer for their assistance in evaluating this paper.

References

Bigg, E. K., C. Leck, and E. D. Nilsson (1996), Sudden changes in arctic atmospheric aerosol concentrations during summer and autumn, *Tellus, Ser. B*, *48*, 254–271.

Bigg, E. K., C. Leck, and L. Tranvik (2004), Particulates of the surface microlayer of open water in the central Arctic Ocean in summer, *Mar. Chem.*, *91*, 131–141.

Clarke, A. D., et al. (1998), Particle nucleation in the tropical boundary layer and its coupling to marine sulfur sources, *Science*, *282*, 89–92.

Covert, D. S., A. Wiedensohler, P. Aalto, J. Heintzenberg, P. H. McMurry, and C. Leck (1996), Aerosol number distribution from 3 to 500 nm diameter in the arctic marine boundary layer during summer and autumn, *Tellus, Ser. B*, *48*, 197–212.

De Haan, D. O., A. L. Corrigan, M. A. Tolbert, J. L. Jimenez, S. E. Wood, and J. J. Turley (2009), Secondary organic aerosol formation by self-reactions of methylglyoxal and glyoxal in evaporating droplets, *Environ. Sci. Technol.*, *43*, 8184–8190.

Facchini, M. C., et al. (2008), Primary submicron marine aerosol dominated by insoluble organic colloids and aggregates, *Geophys. Res. Lett.*, *35*, L17814, doi:10.1029/2008GL034210.

Heintzenberg, J., and C. Leck (1994), Seasonal variation of the atmospheric aerosol near the top of the marine boundary layer over Spitsbergen related to the Arctic sulphur cycle, *Tellus, Ser. B*, *46*, 52–67.

Heintzenberg, J., and C. Leck (2012), The summer aerosol in the central Arctic 1991-2008: Did it change or not? *Atmos. Chem. Phys.*, *12*, 3969–3983.

Heintzenberg, J., C. Leck, W. Birmili, B. Wehner, M. Tjernström, and A. Wiedensohler (2006), Aerosol number-size distributions during clear and

fog periods in the summer high Arctic, 1991, 1996 and 2001, *Tellus, Ser. B*, *58*, 341–359.

Held, A., I. M. Brooks, C. Leck, and M. Tjernström (2011), On the potential contribution of open lead particle emissions to the central Arctic aerosol concentration, *Atmos. Chem. Phys.*, *11*, 3093–3105, doi:10.5194/acp-11-3093-2011.

Karl, M., A. Gross, C. Leck, and L. Pirjola (2011), A new flexible multicomponent model for the study of aerosol dynamics in the marine boundary layer, *Tellus, Ser. B*, *63*, 1001–1025.

Karl, M., C. Leck, A. Gross, and L. Pirjola (2012), A study of new particle formation in the marine boundary layer over the central Arctic Ocean using a flexible multicomponent aerosol dynamic model, *Tellus, Ser. B*, *64*, 17,158, doi:10.3402/tellusb.v17164i17150.17158.

Kozyrev, A. V., and A. G. Sitnikov (2003), Evaporation of charged drops, *Russ. Phys. J.*, *46*, 646–655.

Kulmala, M., and V.-M. Kerminen (2008), On the growth of atmospheric nanoparticles, *Atmos. Res.*, *90*, 132–150.

Kulmala, M., et al. (2013), Direct observations of atmospheric aerosol nucleation, *Science*, *339*, 943–946.

Kupiszewski, P., et al. (2013), Vertical profiling of aerosol particles and trace gases over the central Arctic Ocean during summer, *Atmos. Chem. Phys. Discuss.*, *13*, 10,395–10,461, doi:10.5194/acpd-13-10395-2013.

Leck, C., and E. K. Bigg (1999), Aerosol production over remote marine areas - A new route, *Geophys. Res. Lett.*, *26*, 3577–3580.

Leck, C., and E. K. Bigg (2008), Comparison of sources and nature of the tropical aerosol with the summer High Arctic aerosol, *Tellus, Ser. B*, *60*, 118–126.

Leck, C., and E. K. Bigg (2010), New particle formation of marine biological origin, *Aerosol Sci. Technol.*, *44*, 570–577.

Leck, C., and C. Persson (1996), Seasonal and short-term variability in dimethylsulfide, sulfur dioxide and biogenic sulfur and sea salt aerosol particles in the Arctic marine boundary layer during summer and autumn, *Tellus, Ser. B*, *48*, 272–299.

Lehtinen, K. E. J., and M. Kulmala (2003), A model for particle formation and growth in the atmosphere with molecular resolution in size, *Atmos. Chem. Phys.*, *3*, 251–257.

Mårtensson, E. M., E. D. Nilsson, G. de Leeuw, L. H. Cohen, and H.-C. Hansson (2003), Laboratory simulations and parameterizations of the primary marine aerosol production, *J. Geophys. Res.*, *108*(D9), 4297, doi:10.1029/2002JD002263.

Orellana, M. V., P. Matrai, C. Leck, C. D. Rauschenberg, A. M. Lee, and E. Coz (2011), Marine microgels as a source of cloud condensation nuclei in the high Arctic, *Proc. Natl. Acad. Sci. U. S. A.*, *108*(33), 13,612–13,617.

Ovadnevaite, J., et al. (2011), Primary marine organic aerosol: A dichotomy of low hygroscopocity and high CCN activity, *Geophys. Res. Lett.*, *38*, L21806, doi:10.1029/2011GL048869.

Pandis, S., J. H. Seinfeld, and C. Pilinis (1990), The smog-fog-smog cycle and acid deposition, *J. Geophys. Res.*, *95*, 18,489–18,500.

Russel, L. M., L. N. Hawkins, A. A. Frossard, P. K. Quinn, and T. S. Bates (2010), Carbohydrate-like composition of submicron atmospheric particles and their production from ocean bubble bursting, *Proc. Natl. Acad. Sci. U. S. A.*, *107*(15), 6652–6657.

Tjernström, M., et al. (2013), The Arctic Summer Cloud-Ocean Study (ASCOS): Overview and experimental design, *Atmos. Chem. Phys. Discuss.*, *13*, 13,541–13,652, doi:10.5194/acpd-13-13541-2013.

Verdugo, P. (2012), Marine microgels, *Annu. Rev. Mar. Sci.*, *4*, 375–400.